

High-Radiation and High-Density Experiments in JT-60U

H. Kubo, S. Sakurai, N. Asakura, S. Konoshima, H. Tamai, S. Higashijima, A. Sakasai, H. Takenaga, K. Itami, K. Shimizu, T. Fujita, Y. Kamada, Y. Koide, H. Shirai, T. Sugie, T. Nakano, N. Oyama, H. Urano 1), T. Ishijima 2), K. W. Hill 3), D. R. Ernst 3), A. W. Leonard 4), the JT-60 Team

Japan Atomic Energy Research Institute, Naka Fusion Research Establishment,
Naka-machi, Naka-gun, Ibaraki-ken, 311-0193, Japan

1) Graduate School of Engineering, Hokkaido University, Sapporo, 060-8628, Japan

2) Graduate School of Engineering, Nagoya University, Nagoya, 464-8603, Japan

3) Princeton Plasma Physics Laboratory, P.O. Box 451, Princeton, NJ 08543, USA

4) General Atomics, P. O. Box 85608, San Diego, CA, 92186-5608, USA

E-mail: kubo@naka.jaeri.go.jp

Abstract. In order to obtain confinement improved plasmas with high radiation at high density, Ar gas was injected into ELMy H-mode plasmas in JT-60U. A confinement improvement of $HH_{98(y,2)} \sim 1$ was obtained with a high radiation loss power fraction ($\sim 80\%$) at an electron density of $\sim 0.65 n_{GW}$. The HH-factor was about 50% higher than that in plasmas without Ar injection.

1. Introduction

The ITER FEAT design requires ELMy H-mode plasmas ($HH_{98(y,2)} = 1$, where $HH_{98(y,2)}$ is the ratio of the thermal energy confinement time to the thermal energy confinement time described by IPB98(y,2) scaling) with a high radiation loss power fraction ($P_{rad}^{tot} / P_{heat}^{tot} \sim 0.8$, where P_{rad}^{tot} is the total radiation loss power and P_{heat}^{tot} is the total heating power) at high density ($n_e / n_{GW} = 0.85$, where n_e is the electron density and n_{GW} is the Greenwald density limit) [1]. However, the confinement is degraded in the high density range in large tokamaks [2,3], and this degradation is a critical issue for the ITER FEAT design. The high radiation loss power fraction is needed for mitigating the severe problem of concentrated power loading of the divertor plates. Controlled injection of impurity gases is a promising technique for enhancement of radiation loss power, either in the main chamber or in the divertor [4-8]. In ITER-FEAT, Ar injection is being considered to enhance the radiative loss power [1]. By injecting impurities, confinement has been improved with high radiation loss power in the high density range in TEXTOR (RI-mode) in a limiter configuration [9]. Confinement improvement due to impurity injection and the formation of a radiating mantle have also been reported in DIII-D in a divertor configuration [10]. A reduction in the ion temperature gradient mode by impurity injection is thought to be a candidate for explaining the improvement [11-13].

In ELMy H-mode plasmas of JT-60U, confinement degradation at high density has been a significant problem [2]. High-radiation and high-density ELMy H-mode plasmas have been investigated using Ne injection into the divertor region in JT-60U [6,7]. By injecting Ne, the confinement was improved by $\sim 15\%$ at $\bar{n}_e \sim 0.65 n_{GW}$. Recently, Ar, which is being considered for injection into ITER-FEAT, has been injected into the main chamber for confinement improvement and radiation loss enhancement due to a radiating mantle at high density. This paper presents the properties of confinement improvement at the pedestal and core plasmas and radiation loss enhancement in the ELMy H-mode discharges with Ar injection.

2. Experiment

Argon gas was injected into ELMy H-mode plasmas (plasma current: 1.2 MA, toroidal magnetic field: 2.5 T, elongation: 1.4, triangularity: 0.36, safety factor at the 95% flux surface: 3.4, n_{GW} : $5.2 \times 10^{19} \text{ m}^{-3}$, neutral beam (NB) injection power: 16 - 20 MW) [14]. JT-60U has a W-shaped divertor at the bottom. Deuterium gas was puffed into the main chamber from the top, and Ar gas into the main chamber from the lower outside in order to form a radiating mantle in the edge region of the main plasma. Neutral particles in the divertor were pumped from the private flux region through exhaust slots near both the inner and outer strike points. The time constant of exhaust for Ar was ~ 0.5 s in the high-density ELMy H-mode discharges. In some discharges, the radiation loss power from the edge region ($r/a > 0.55$) was controlled with a feedback technique using Ar puffing. With the feedback control, quasi-stationary ELMy H-mode plasmas were sustained in the region of $P_{\text{rad}}^{\text{tot}} < 0.8 P_{\text{net}}$, where P_{net} is the net heating power.

3. Results and Discussion

Waveforms of ELMy H-mode plasmas without and with Ar injection are shown in Fig. 1. NB with a power of ~ 16 MW is injected. Without Ar injection, an intense D_2 gas puff is necessary to increase the electron density. As the electron density increases with the D_2 gas puff, the stored energy decreases. An X-point MARFE appears at 7.3 s, and the radiation loss power increases in the divertor plasma. The radiation loss power in the main plasma, however, remains constant and low. The D_α line intensity increases with the D_2 gas puff. In the discharge with Ar injection, the radiation loss power from the edge plasma $P_{\text{rad}}^{\text{edge}}$ is controlled with a feedback technique by the Ar gas puff rate. As seen in the bottom frame, the $P_{\text{rad}}^{\text{edge}}$ is well controlled near the reference value by changing the Ar puffing rate. In discharges with Ar injection, the D_2 gas puffing rate to increase the electron density becomes low. It might be attributed to improvement of particle confinement. In this discharge, without D_2 gas puffing, the electron density is increased by beam fueling and

recycling. In high density range, the stored energy is maintained at a high level. The D_α line intensity remains low, and type-I ELMs are maintained. The radiation loss power from the main plasma increases to the same level as the radiation loss power from the divertor plasma.

The ratio of the total radiation loss power to the net heating power $P_{\text{rad}}^{\text{tot}} / P_{\text{net}}$ (radiated power fraction) and the ratio of the radiation loss power from the main plasma to the total radiation loss power $P_{\text{rad}}^{\text{main}} / P_{\text{rad}}^{\text{tot}}$ are compared for different Ar densities in Fig. 2. The radiated power fraction is $\sim 45\%$ in plasmas without Ar injection at $\bar{n}_e \sim 0.5 n_{\text{GW}}$. At $\bar{n}_e > 0.5 n_{\text{GW}}$, a radiation band (MARFE) of carbon line emission is found near the

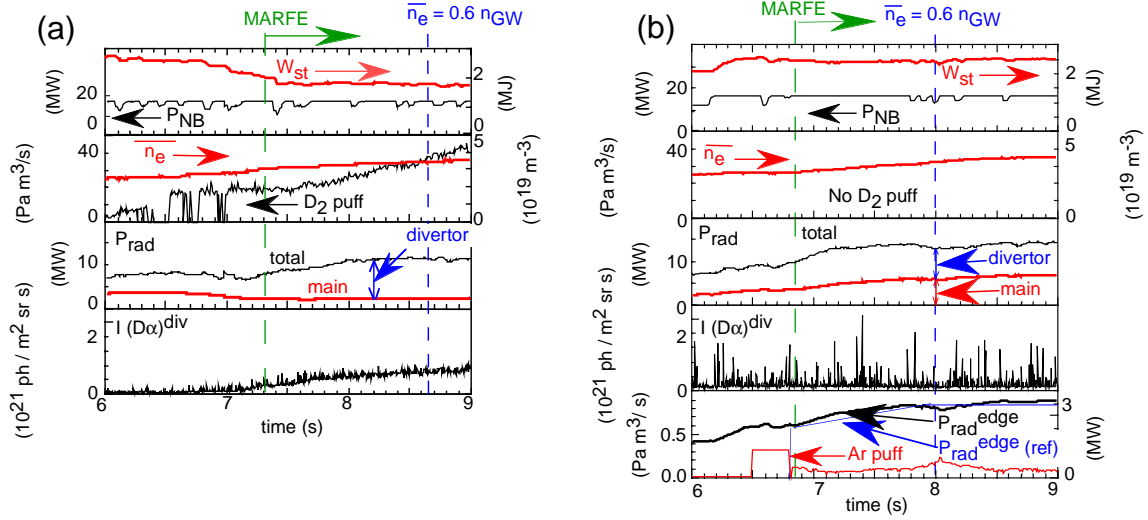


Fig. 1. Waveforms of ELMy H-mode plasmas (a) without and (b) with Ar injection. P_{NB} : NBI power, W_{st} : stored energy, \bar{n}_e : line-averaged electron density, D_2 puff: puffing rate of deuterium gas, P_{rad} : total radiation loss power and radiation loss power from the main plasmas, $I(D_\alpha)^{\text{div}}$: intensity of D_α line emission from the divertor plasmas, Ar puff: puffing rate of Ar gas, $P_{\text{rad}}^{\text{edge}}$: radiation loss power from the edge plasma, and $P_{\text{rad}}^{\text{edge}}(\text{ref})$: reference for feedback control of the $P_{\text{rad}}^{\text{edge}}$.

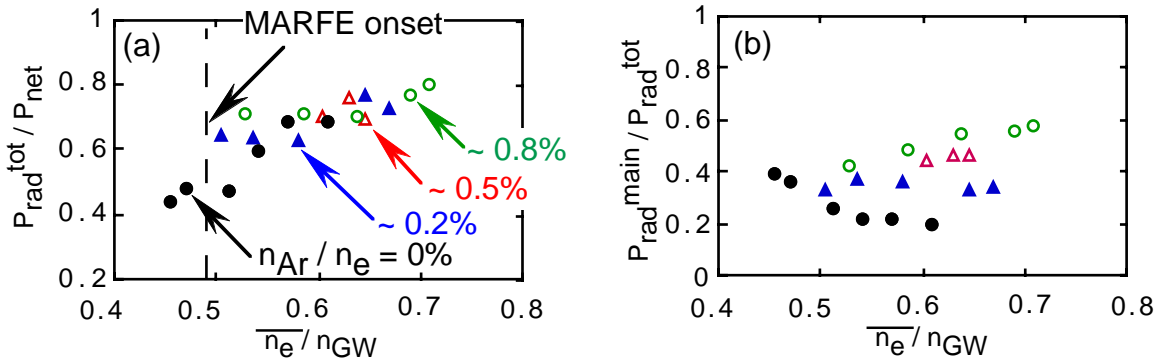


Fig. 2. (a) Ratio of the total radiation loss power to the net heating power, and (b) ratio of the radiation loss power from the main plasma to the total radiation loss power for different Ar densities against the electron density normalized by the Greenwald density limit. Here, the total radiation loss power is the sum of the main plasma radiation loss power and the divertor plasma radiation loss power.

null point in all cases (both with and without Ar injection). The radiated power fraction in the case without Ar increases with the electron density, since the radiation loss power from the divertor increases due to increased radiation loss power from the MARFE. The radiation loss from the divertor becomes dominant as seen in Fig. 2 (b). The total radiation loss power increases also with the electron density in the plasmas with Ar injection. As the Ar density increases, the $P_{\text{rad}}^{\text{main}} / P_{\text{rad}}^{\text{tot}}$ fraction increases, and the radiation loss from the main plasma becomes dominant. In the plasmas with Ar injection, the radiation loss power due to the MARFE does not increase with the electron density. As a result, the $P_{\text{rad}}^{\text{tot}} / P_{\text{net}}$ in the case with Ar injection is about the same as that without Ar injection. By control of the Ar density, the $P_{\text{rad}}^{\text{main}} / P_{\text{rad}}^{\text{tot}}$ fraction can be changed. At $\bar{n}_e = 0.65 n_{\text{GW}}$, the total radiated power fraction reaches $\sim 80\%$ relative to the net heating power.

The HH-factor ($\text{HH}_{98}(y, 2)$) [15] is plotted for different Ar densities against the electron density in Fig. 3 (a). In the plasma without Ar injection, the HH-factor decreases from 0.9 to 0.6 as the $\bar{n}_e / n_{\text{GW}}$ ratio increases from 0.45 to 0.60. On the other hand, the HH-factor is kept high in the plasma with Ar injection. When the Ar density is higher than 0.5%, the HH factor remains near unity in the range of $\bar{n}_e < 0.65 n_{\text{GW}}$. The HH-factor was about 50% higher than that in plasmas without Ar injection at $\bar{n}_e = 0.65 n_{\text{GW}}$. An Ar concentration of 0.5% corresponds to about a 9% reduction in the ion density. In JT-60U, the dominant intrinsic impurity is carbon. The carbon density is about 5% in the discharges, and it is not changed by Ar injection. Therefore, the improvement in confinement more than compensated for the deuterium density reduction by impurity contamination, resulting in higher neutron production rates. The confinement improvement by Ar injection is higher

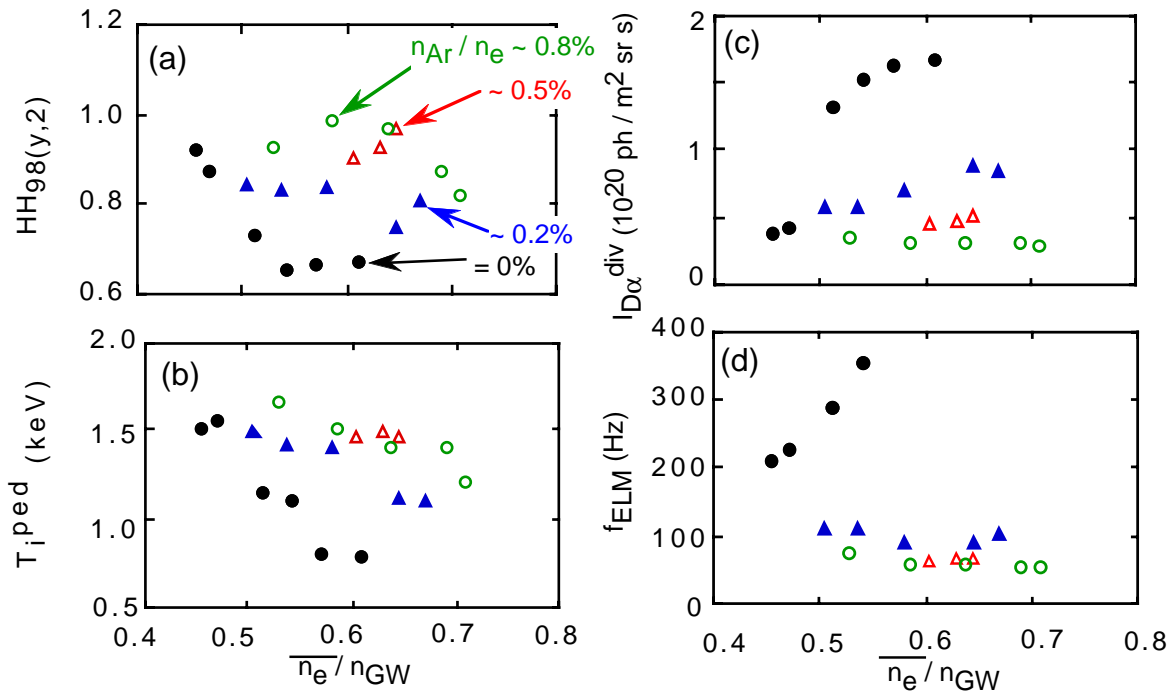


Fig. 3. (a) HH-factor, (b) ion temperature at the pedestal, (c) $D\alpha$ line intensity in the divertor plasmas, and (d) type-I ELM frequency for different Ar densities against electron density.

than that by Ne injection ($\sim 15\%$) [6,7].

In the following three paragraphs, we discuss the characteristics of the confinement improvement with Ar injection. The main plasma parameter profiles (P_{rad} , n_e , T_e , T_i) with and without Ar injection are compared at $\bar{n}_e = 0.6 n_{\text{GW}}$ in Fig. 4. The total radiation loss fractions for the cases with and without Ar injection are 67% and 77%, respectively. In the plasma with Ar injection, while the radiative loss power is predominantly enhanced in the edge region, the power radiated from the region of $\rho/a < 0.6$ is $\sim 10\%$ of the heating power injected into the region. The electron density profile in the plasma with Ar injection is similar to the profile in the plasma without Ar injection. Compared with the plasma without Ar injection, in the plasmas with Ar injection, the electron and ion temperatures are higher at the pedestal, and the gradients of the temperatures are higher in the core region. Therefore, the confinement is improved in both the pedestal and core regions. The RI-mode plasmas in TEXTOR have an L-mode edge structure, and a peaked electron density profile [9]. Therefore, the present confinement improvement due to Ar injection is different from that for the RI-mode in TEXTOR.

Here, we compare the pedestal structure between the cases with and without Ar injection. Ion temperature profiles in the edge regions are shown in Fig. 5. As the electron density increases, the pedestal width of the ion temperature decreases. At high density, the pedestal in the plasma with Ar injection is wider than that in the plasma without Ar injection. Figure 3 (b) illustrates that the ion temperature at the pedestal decreases as the electron density increases in the case without Ar injection. However, with Ar injection, the ion temperature remains rather high even in the high density range. The D_α line intensity and type-I ELM frequency are shown in Fig. 3 (c) and (d), respectively. In the plasma

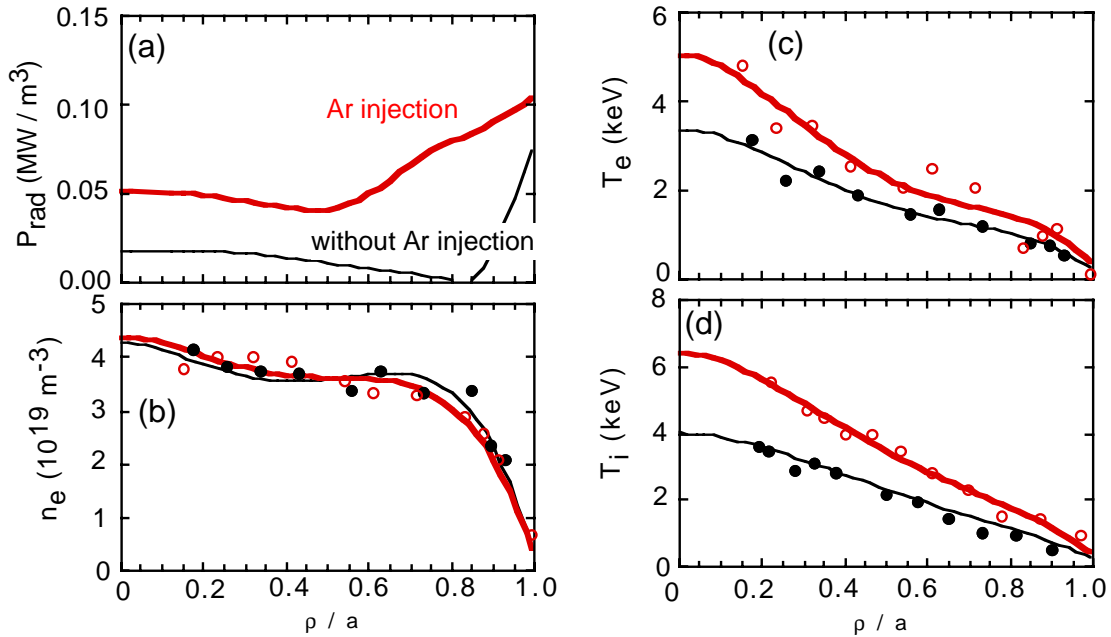


Fig. 4. Profiles of (a) radiation loss power density, (b) electron density, (c) electron temperature, and (d) ion temperature in ELMy H-mode plasmas with and without Ar injection.

without Ar injection, the D_α line intensity increases with the electron density due to an intense gas puff needed to increase the electron density. As the electron density increases from 0.45 to 0.55 n_{GW} , the ELM frequency increases from 200 to 380 Hz. At $\bar{n}_e \sim 0.55 n_{GW}$, the ELMs appear to change from type-I to type-III. This change might be attributed to decrease in the electron temperature [16]. In other tokamaks, similar phenomena (increase in the ELM frequency and change from a type-I ELM phase to a type-III ELM phase) have also been observed with D_2 gas puffing [3,17]. However, the ELM frequency decreases with Ar injection. The regular type-I ELM is maintained even at high density. The frequency is slightly lower ($\sim 40\%$) in the case with Ar density of 0.5% than in the case with Ar density of 0.2%. Figure 6 shows time evolutions of Ar XV 22.1 nm line intensity, radiation loss power from the main plasma, and the maximum surface temperature of the outer divertor plates just after the start of Ar gas injection. The ELM frequency changes from ~ 120 to ~ 70 Hz in a short period (~ 0.2 s) after the start of Ar injection. At that time, the increase in the radiation loss power is still small ($\sim 0.02 P_{net}$). Therefore, the decrease in the ELM frequency cannot be explained by an increase in reheating time due to a decrease in the edge heating power. In ASDEX, a similar immediate decrease in ELM frequency has been observed following Ne injection, where the loss of stored energy per ELM (ΔW_{ELM}) increased, but the average energy loss ($f_{ELM} \Delta W_{ELM}$) did not change significantly [17].

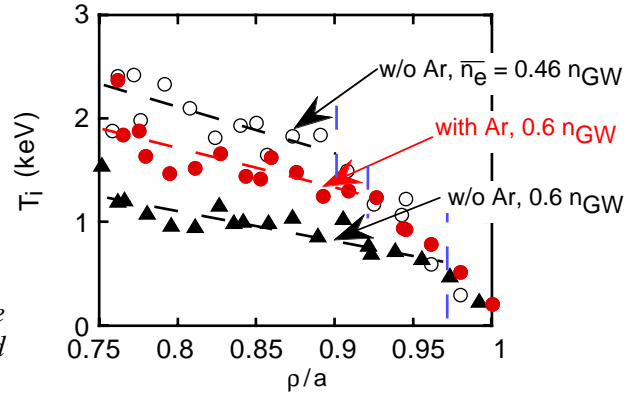


Fig. 5. Ion temperature profiles in the edge regions of ELMy H-mode plasmas with and without Ar injection.

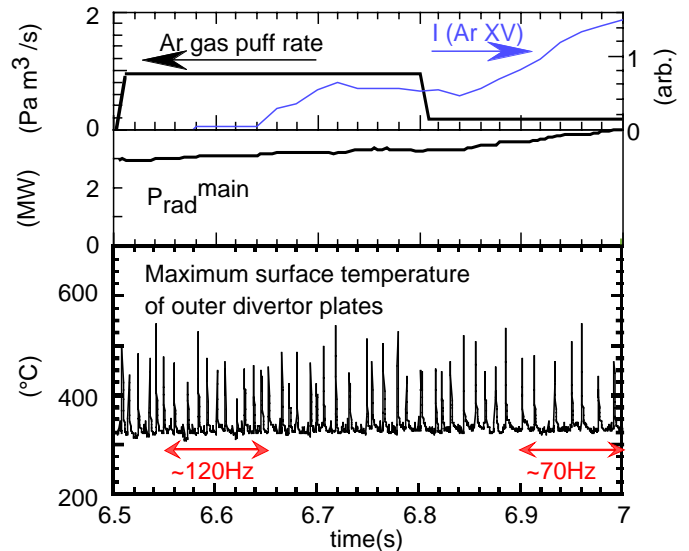


Fig. 6. Time evolutions of Ar gas puffing rate, Ar XV 22.1 nm line intensity, radiation loss power from the main plasma, and the maximum surface temperature of the outer divertor plates.

However, in the present experiment, it is suggested by the time evolution of the maximum surface temperature of the outer divertor plates that the energy loss due to an ELM does not change significantly [14].

As shown in Fig. 4, with Ar injection the confinement is also improved in the core region. A relation between the core plasma confinement and the ion temperature at the pedestal has been found in some tokamaks [18-21]. In Fig. 7, the HH-factor is plotted against the ion temperature at the pedestal for different Ar densities. The HH-factor seems to increase consistently with the ion temperature even for different Ar densities. The confinement improvement in the core plasma with Ar injection might be related to the high ion temperature at the pedestal. Higher Z_{eff} , as well as increased pedestal ion temperature, may improve core confinement by suppressing toroidal ITG modes. In a parametrization [22] of the toroidal ITG threshold, based on gyrokinetic code results, the critical inverse ion temperature gradient scale length scales as $Z_{\text{eff}}^{0.7}$. This parametrization suggests stability for toroidal ITG modes in the case with Ar, and instability in the case without Ar, over most of the plasma cross-section [23].

Large ELMs are a concern for ITER because of the large transient heat flux to the divertor plates [24]. As seen in Fig. 6, the transient heat load due to ELMs cannot be reduced by injecting Ar. However, the frequency is reduced by a factor of two. Therefore, the time averaged heat load due to ELMs is reduced. This observation suggests that the erosion of the divertor plates can be mitigated by impurity injection.

At $\bar{n}_e > 0.75 \text{ n}_{\text{GW}}$, the present improved confinement by Ar injection has not been obtained in JT-60U [14]. The reason seems to be difficulty in controlling the radiation loss power in the high density range. At high density, even a little excessive Ar puff enhances the radiative loss power from the main plasma too much. In this case, the main plasma radiation loss enhanced by Ar injection causes a decrease in the electron temperature, and the decrease in the electron temperature results in more radiation loss enhancement because of high radiation loss coefficients of Ar at low temperature. An increase of central heating power is effective for controlling the decrease in the electron temperature. It might be possible to extend the operational range to higher density by increasing the central heating power and controlling the radiation loss power carefully.

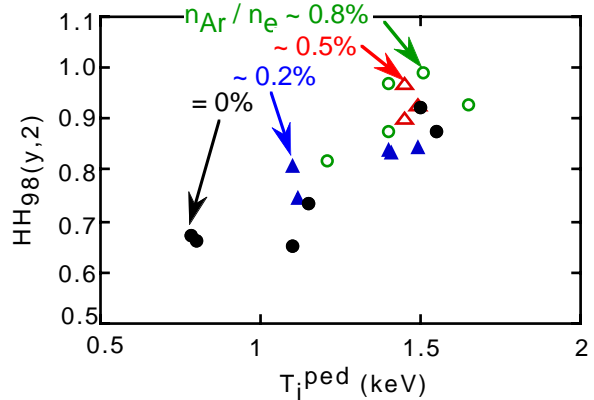


Fig. 7. Relation between the HH-factor and the ion temperature at the pedestal for different Ar densities.

4. Conclusions

In ELMy H-mode discharges, Ar injection was effective for obtaining high confinement with high radiation loss power at high density. At an electron density of $\sim 0.65 n_{GW}$, the HH-factor in the plasma with Ar injection was about 50% higher than the HH-factor in plasmas without Ar injection. The improvement in confinement more than compensated for the deuterium density reduction by impurity contamination, resulting in higher neutron production rates. The confinement was improved in both the pedestal and core regions. The confinement improvement seemed to be closely related to the high ion temperature at the pedestal. It might be possible to extend the operational range to higher density by increasing the central heating power and controlling the radiation loss power carefully.

References

- [1] INTERNATIONAL ATOMIC ENERGY AGENCY, "Technical basis for the ITER-FEAT outline design", to be published in ITER Documentation Series, IAEA, Vienna.
- [2] ASAKURA, N., et al., Plasma Phys. Control. Fusion **39** (1997) 1295.
- [3] JET TEAM, Nucl. Fusion **39** (1999) 1687.
- [4] SAMM, U., et al., Plasma Phys. Control. Fusion **35** (1993) B167.
- [5] GRUBER, O. et al., Phys. Rev. Lett., **74** (1995) 4217.
- [6] ITAMI, K., et al., Fusion Energy 1997 (Proc. 16th Int. Conf. Montreal, 1996), Vol. 1, IAEA, Vienna (1996) 385.
- [7] ITAMI, K., et al., J. Nucl. Mater. **266-269** (1999) 1097.
- [8] MATTHEWS, G. F., et al., Nucl. Fusion **39** (1999) 19.
- [9] WEYNANTS, R. R., Nucl. Fusion **39** (1999) 1637.
- [10] JACKSON, G. L., et al., J. Nucl. Mater. **266-269** (1999) 380.
- [11] HILL, K. W., et al., Nucl. Fusion **39** (1999) 1949.
- [12] McKEE, G., et al., Phys. Rev. Lett. **84** (2000) 1922.
- [13] BOEDO, J., A., Nucl. Fusion **40** (2000) 209.
- [14] SAKURAI, S., et al., to be published in Nucl. Mater.
- [15] ITER Physics Expert Groups on Confinement and Transport and Confinement Modelling and Database, Nucl. Fusion **39** (1999) 2175.
- [16] IGITKHANOV, Yu., et al., Contrib. Plasma Phys. **40** (2000) 368.
- [17] SUTTROP, W., et al., Plasma Phys. Control. Fusion **40** (1998) 771.
- [18] GREENWALD M., et al., Nucl. Fusion **37** (1997) 793.
- [19] SUTTROP, W., et al., Plasma Phys. Control. Fusion **39** (1997) 2051.
- [20] URANO, H., et al., to be published in Plasma Phys. Control. Fusion.
- [21] JANESCHITZ, G., et al., (Proc. 26th EPS Conf. on Control. Fusion and Plasma Phys. Maastricht, 1999), vol. **23J**, EPS, Geneva (1999) 1445.
- [22] KOTSCHENREUTHER, M., et al., Phys. Plasma **2** (1995) 2381.
- [23] ERNST, D., R., et al., Fusion Energy 1998 (Proc. 17th Int. Conf. Yokohama, 1998), Vol. 2, IAEA, Vienna (1999) 741.
- [24] LEONARD, A. W., et al., J. Nucl. Mater. **266-269** (1999) 109.